UNPUBLISHED PRELIMINARY DATA

UARI Research Report No. 8

28 p.

HYPERSONIC FLOW WITH NON-EQUILIBRIUM DISSOCIATION AROUND BLUNT BODIES IN FLOW FACILITIES AND IN FREE FLIGHT

(UARI Research Report No. 8)

N64 13055

CODE-1
NASA CR 55138

by

RUDOLF HERMANN
JANARDANARAO YALAMANCHILI (Ph. D. Thesis)

Oct. 1963 28 p refs

(NASA Grant NsG-381)
(NASA CR-55138) OTS: $2.60 ph, $1.04 mf

This report contains material from the Doctoral Thesis of the junior author.

This research work is partially supported by the National Aeronautics and Space Administration under research grant NsG-381.

Paper presented by R. Hermann at the Annual Meeting of the WISSENSCHAFTLICHE GESELLSCHAFT FUR LUFT- UND RAUMFAHRT, at Munich, Germany, October 8 - 12, 1963

UNIVERSITY OF ALABAMA RESEARCH INSTITUTE,
HUNTSVILLE, ALABAMA

OCTOBER, 1963

OTS PRICE
XEROX $ 2.60 ph.
MICROFILM $ 1.04 mf.

UARI Research Report No. 8

HYPERSONIC FLOW WITH NON-EQUILIBRIUM DISSOCIATION AROUND BLUNT BODIES IN FLOW FACILITIES AND IN FREE FLIGHT

by

RUDOLF HERMANN
JANARDANARAO YALAMANCHILI

This report contains material from the Doctoral Thesis of the junior author.

This research work is partially supported by the National Aeronautics and Space Administration under research grant NsG-381.

Paper presented by R. Hermann at the Annual Meeting of the
WISSENSCHAFTLICHE GESELLSCHAFT FÜR LUFT- UND RAUMFAHRT
at Munich, Germany, October 8 - 12, 1963

UNIVERSITY OF ALABAMA RESEARCH INSTITUTE

HUNTSVILLE, ALABAMA

OCTOBER, 1963

HYPERSONIC FLOW WITH NON-EQUILIBRIUM DISSOCIATION AROUND BLUNT BODIES IN FLOW FACILITIES AND IN FREE FLIGHT**

by Rudolf Hermann
Janardanarao Yalamanchili*

1. INTRODUCTION

During re-entry of an aero-space vehicle into the atmosphere high stagnation temperatures and velocities corresponding to about Mach number 25 are encountered. Above Mach number 5 or 6, air no longer behaves as a perfect gas and molecular vibration, dissociation and ionization occurs. It is a pleasure to refer to my paper on hypersonic re-entry given at the 1961 Annual Meeting of the WGL at Freiburg, ref. 1. Among other subjects I had discussed dissociation of air, with the individual reactions, the characteristic temperature for dissociation, and the equilibrium "constants" for oxygen and nitrogen. The "constants" are actually strong functions of the temperature. I introduced a so-called simplified air model, which consists of oxygen and nitrogen only. Also, only dissociation of each component is considered, while chemical reactions between oxygen and nitrogen are neglected. In addition, the following physical fact suggests further simplification. If, at a given pressure, the temperature is raised, the oxygen begins to dissociate first and the fraction of oxygen dissociated increases with temperature. All the while the nitrogen stays practically intact as molecules. Only after the temperature is raised to the point where the oxygen is fully (say 99%) dissociated, does the dissociation of nitrogen begin. This means a separation of the two processes, which leads to two separate quadratic equations for the degree of dissociation α of oxygen and the degree of dissociation β for nitrogen as function of temperature and pressure. The comparison of degrees of dissociation obtained by this simplified model with so-called "exact" results calculated for many air components and many reactions by large computers, was very gratifying. Hence, we will use the simplified model also in the present investigation.

* University of Alabama Research Institute, Huntsville, Alabama

** This report contains material from the Doctoral Thesis of the junior author. Partial support for the Research was given by the National Aeronautics and Space Administration, NsG-381. The authors acknowledge the assistance of J. Thoenes.
Details of the subjects treated here are found in Ref. 12.

An illustrative survey of the happenings during re-entry with respect to dissociation is given in Figure 1, taken from ref. 1. Dissociation of oxygen and nitrogen at the stagnation point of a vehicle is given in an altitude versus velocity diagram. Also included are re-entry trajectories for various ballistic vehicles and for one glide vehicle. This diagram illustrates very well the fact that the dissociation of oxygen and nitrogen are separated from each other. There are two important restrictions in the graph. First, the dissociation values given are valid at the stagnation point only for the respective vehicle. Second, the values are calculated for equilibrium conditions, that means assuming that the flow has sufficient time to adjust to its chemical composition due to the prevailing stagnation pressure and temperature conditions. The difference between equilibrium and non-equilibrium flow was also mentioned in the Freiburg paper. In addition several examples had been calculated for equilibrium conditions for hypersonic flow around a sphere for Mach number 7 and 10 for wind tunnel supply temperature between 2700°K and 4400 °K. It was pointed out that the flow data were not a solution of the exact equation but a tentative approximation assuming a Newtonian pressure distribution and a linear velocity distribution to an assumed sonic point. From this, the other flow parameters, α, T, ρ, were calculated by the energy equation.

In the present report we will consider flow with oxygen dissociation in non-equilibrium. That means we have to make use of the "rate equation" which expresses the fact that finite time is needed for the dissociation process and the recombination process. We will first investigate the flow through a hypersonic nozzle up to a Mach number of about 15 for various supply conditions, nozzle geometries and sizes. Afterwards we will investigate the flow around a cylinder (two-dimensional case) which is placed in a wind tunnel stream with frozen dissociation of oxygen. We will study the effect on the shock shape and detachment distance, and on the other flow parameters up to the sonic point.

2. Some Aspects of Real Gas Effects: The Equation of State, Energy Equation, and Degree of Dissociation Rate Equation.

2.1 Basic Assumptions

The model of the air being used consists only of oxygen and nitrogen. The temperature range considered is such that only dissociation of oxygen but no dissociation of nitrogen occurs. Also, chemical reactions between O and N and ionization are neglected.

where the mole fractions f_i are for the three species indicated. The internal energies of the O_2 and N_2 molecules consists of translational, rotational, and vibrational energies of the molecules. The energy of the oxygen atom is simply translational energy. This yields the equations

$$E_O = (3/2)\ \frac{\hat{R}T}{M} \tag{6}$$

$$E_{O2} = (5/2)\ \frac{\hat{R}T}{M} + \frac{2270\ (^oK)\ \frac{\hat{R}}{M}}{Exp(2270/T) - 1} \tag{7}$$

$$E_{N2} = (5/2)\ \frac{\hat{R}T}{M} + \frac{3390\ (^oK)\ \frac{\hat{R}}{M}}{Exp\ (3390/T) - 1} \tag{8}$$

where vibrational constant (θ_v) is 2270°K for oxygen and 3390°K for nitrogen, $\hat{R}$ universal gas constant. D is the dissociation energy per mole for oxygen. Substituting the values for E_i and f_i and D, we obtain the expression for the enthalpy

$$h = R\left\{3/2(.4227)\,\alpha\ T + .211\ (1 - \alpha)\left[5/2\ T + \frac{2270(^oK)}{Exp(2270/T) - 1}\right]\right.$$
$$\left. + .789\left[5/2\ T + \frac{3390(^oK)}{Exp(3390/T) - 1}\right] + .211\,\alpha\ 59000(^oK)\right\}$$
$$+ R(1 + .211\,\alpha\ )T \tag{9}$$

Comparing this complicated equation for the enthalpy with the enthalpy equation for a perfect gas shows the added complexity to our problem.

The energy equation expresses the preservation of kinetic energy and enthalpy per unit mass or

$$\frac{u^2}{2} + h = h_t \tag{10}$$

2.4 Rate Equation

In the process of dissociation, the oxygen molecule must collide with another particle either in the atomic or molecular state. The dissociation reaction is described by

$$O_2 + M \xrightarrow{k_d} 2O + M \tag{11}$$

Here M is the third body which is either an oxygen atom, oxygen molecule or nitrogen molecule in this investigation. The change in the number of oxygen atoms per second is positive and can be expressed by

$$\left(\frac{d\,(n_0')}{dt}\right)_{diss} = k_d\, n_{02}'\, n_M' \qquad (12)$$

The recombination process is the inverse of the dissociation. In order to occur it is necessary that two oxygen atoms collide at the same time with a third body which is able to carry away the energy in such a way that two atoms can form a stable diatomic oxygen molecule. The reaction can be written as

$$0 + 0 + M \xrightarrow{k_r} 0_2 + M \qquad (13)$$

The change in the number of oxygen atoms per second for this reaction is negative and can be expressed by

$$\left(\frac{d\,(n_0')}{dt}\right)_{recomb} = -k_r\, n_0'^{\,2}\, n_M' \qquad (14)$$

If a gas is in equilibrium the dissociation rate is equal and opposite to the recombination rate and hence the net rate is zero. For this combination the so called "Pressure Equilibrium Constant" K_p is defined, which was discussed in the Freiburg paper and there denoted by K. The corresponding values for oxygen and nitrogen dissociation were denoted by K_α, and K_β. The K_p has the dimension of a pressure (in atmospheres) and hence is referred to as "pressure" equilibrium constant. It is advantageous to define a so-called "concentration" equilibrium constant K_e which is related to K_p by

$$K_e = \frac{K_p}{RT}\ , \qquad (15)$$

with the dimension particles per unit volume. In the above equations, n_{02}' and n_0' are the number of particles per unit volume of the species 0_2 and 0, and n_M' is the number of particles acting as a third body per unit volume. Obviously

$$n_M' = n_0' + n_{02}' + n_{N2}' \qquad (16)$$

In non-equilibrium flow the net rate between dissociation and recombination is not zero and we can express the number w of oxygen atoms liberated per unit volume and per unit time as the sum of the dissociation and the recombination rate, yielding

$$w = C\rho u \frac{d\alpha}{dx} = \left(\frac{dn_0'}{dt}\right)_{diss} + \left(\frac{dn_0'}{dt}\right)_{recomb} \qquad (17)$$

Using the above equations, the change of the degree of dissociation along a stream line, can be expressed by

$$\rho u C \frac{d\alpha}{dx} = k_d(n_{02}')(n_M') - k_r(n_O')^2(n_M') \qquad (18)$$

and after some simplification we obtain

$$u \frac{d\alpha}{dx} = (1 + 0.211\alpha) \left[B_1 k_d \rho (1 - \alpha) - B_2 k_r \rho^2 \alpha^2\right] \qquad (19)$$

where B_1 and B_2 designate certain constants. It is important to see that the dissociation process is proportional to the density and the available oxygen molecules while the recombination process is proportional to the square of the density and the square of the oxygen atoms already dissociated.

In order to calculate flow processes we have to know the numerical values of k_d and k_r. They are called rate "constants" but are dependent on temperature. Various theories have predicted the recombination rate constant and its dependence on temperature, however their results vary considerably, up to a factor 1000. After careful comparison of various theories and in particular the consideration of the formula proposed by Vincenti, ref. 2, and Hall, ref. 3, the following equation is used

$$K_r = \frac{6.25 \times 10^{-44} \left[\left(\frac{m^3}{\text{particle}}\right)^2 (^oK)^{\frac{1}{2}} \text{ sec}^{-1}\right]}{T} \qquad (20)$$

The dissociation rate constant k_d is presented graphically in Figure 2 as a function of the inverse temperature from various sources. Their spread of a factor 1000 indicates the uncertainty of our present knowledge and the need for either more experiments and/or analytical calculation. Generally, k_d is calculated from the concentration equilibrium constant K_e and k_r by the relation

$$K_e = \frac{k_d}{k_r} \qquad (21)$$

The k_d values which are used for this investigation are shown in the graph.

The equilibrium constants K_p and K_e are well established. The values of K_e adapted for this study are very close to the ones published by Hansen, ref. 4, and by Glowacki, ref. 5.

3. Flow Through a Hypersonic Nozzle

3.1 Assumptions and Equations

The flow through a hypersonic nozzle has been calculated for one-dimensional flow with the basic assumption specified in part 2 for the real gas effects. In

addition, viscosity, diffusion, and heat conductivity of the air are neglected. Five equations have been established. The continuity equation and the momentum equation in the x direction are of the conventional form and hence are omitted here. In addition, there are the equation of energy, the equation of state, and the rate equation. Those three equations have been described and are listed in part 2. The five unknowns are velocity u, pressure p, temperature T, density ρ, and degree of dissociation α. In addition, the energy equation 10 contains the enthalpy h; but this h is expressed by T and α through equation 9. From the five equations, density ρ and velocity u have been eliminated and three ordinary differential equations have been derived as follows.

$$\frac{d\alpha}{dx} = \frac{C^2 \rho^2 \left(1 + \frac{n_{02}}{n_{02} + n_{N2}}\right) k_r \left[\frac{K_e}{2C} (1 - \alpha) - \rho \alpha^2\right]}{2\left(\frac{n_{02}}{n_{02} + n_{N2}}\right) \left(\frac{\dot{m}}{A^*}\right) \left(\frac{A^*}{A}\right)} \tag{22}$$

$$\frac{d\rho}{dx} = \frac{RZT \left(\frac{A}{A^*}\right)^2 \rho^3 \left[\frac{1}{Z} \left(\frac{n_{02}}{n_{02} + n_{N2}}\right) \frac{d\alpha}{dx} + \frac{1}{T} \frac{dT}{dx} - \left(\frac{A^*}{A}\right) \frac{d}{dx} \left(\frac{A}{A^*}\right)\right]}{\left(\frac{\dot{m}}{A^*}\right)^2 (1 - K)}$$

$$- \rho \left(\frac{A^*}{A}\right) \frac{d}{dx} \left(\frac{A}{A^*}\right)$$

$$\text{where } K = \frac{RZT \rho^2 \left(\frac{A}{A^*}\right)^2}{\left(\frac{\dot{m}}{A^*}\right)^2} \tag{23}$$

$$\frac{dT}{dx} = \frac{(1 - K) \left[\frac{\partial h}{\partial \alpha} - \frac{RT}{1 - K} \left(\frac{n_{02}}{n_{02} + n_{N2}}\right) \frac{d\alpha}{dx} + RZT \left(\frac{A^*}{A}\right) \frac{d}{dx} \left(\frac{A}{A^*}\right)\right]}{RZ - \frac{\partial h}{\partial T} (1 - K)} \tag{24}$$

This system shows the derivatives for α, ρ, and T with respect to x. It is noted that the derivative of α depends only on the state of the gas and the area itself. The derivative of the density contains, besides the state of the gas, the derivatives of α, T, and the area change. The derivative of the temperature contains also derivatives of α and the area change but, in particular, two partial

derivatives of the enthalpy with respect to α and T.

3.2 Flow Calculations

Calculations for both, equilibrium flow and non-equilibrium flow in hypersonic nozzles have been carried out in order to compare the results of the two concepts. Because of the low velocity in the sub-sonic portion of the nozzle, the flow is assumed to be in equilibrium up to the throat in either case. Assuming an isentropic expansion, the temperature, compressibility factor, and the enthalpy can be determined from a Mollier chart for arbitrary values of the pressure. The corresponding density and velocity can then be calculated. The throat conditions can be found by calculating the mass flux as functions of x which must be a maximum at the throat. For the equilibrium calculation in the supersonic portion of the nozzle, the same procedure has been followed. The essential contribution of this investigation is of course the calculation of the non-equilibrium flow. The throat conditions determined by the equilibrium flow calculations represent the initial values for the non-equilibrium flow in the supersonic portion of the nozzle. In addition, in order to start the numerical integration, the derivatives at the throat had to be specified and they were taken to be those of the equilibrium flow. This is justified because of the small interval of integration that was chosen.

In non-equilibrium flow the solution depends on the shape and on the absolute dimensions of the nozzle. Because many hypersonic nozzles are axisymmetric and have an approximate conical shape, the following geometrie has been selected.

$$\frac{A}{A^*} = 1 + \frac{x}{\ell}^2 \tag{25}$$

with the parameter

$$= \frac{d}{2 \tan \chi} \tag{26}$$

where d is the diameter of the throat and χ is the asumptotic angle of the nozzle.

The numerical calculations are done for various values of the parameter ℓ ranging from 0.3464 to 0.8 inches. This covers a family of nozzles with cone angles ranging from 5° to 30°, with throat diameters ranging from 0.06 to 0.8 inches, with a total nozzle length between 35 and 80 inches and with a maximum area ratio of 10,000.

As the shape of the nozzle is specified as function of x, the above system of differential equations is simultaneously solved on a high speed Computer, the IBM 7090, using the so-called third order Runge-Kutta integration method.

3.3 Numerical Results of Hypersonic Nozzle Flow.

Degree of oxygen dissociation α along the hypersonic nozzle is shown in Figure 3 for some characteristic supply pressures and temperatures. Both equilibrium and non-equilibrium flow calculations are shown in the same diagram. For equilibrium flow, the degree of dissociation decreases fast due to the strongly decreasing temperature. In contrast, non-equilibrium flow shows freezing of the degree of dissociation α very soon behind the throat, at an area ratio of 2 to 4. Downstream of it, the degree of the dissociation stays constant within the accuracy of this graph, that is the chemical composition is frozen. At a fixed supply pressure, the frozen dissociation is highest at the higher supply temperature. At a fixed supply temperature, the frozen dissociation decreases with increasing supply pressure.

The freezing of the chemical composition just downstream of the throat was already observed by Bray for Lighthill's "ideally dissociated gas". This can be explained by the fact that dissociation and recombination processes, which are balanced in the reservoir due to equilibrium conditions, decrease at different rates as the air expands. In particular, the rate of dissociation tends to zero first, decreasing strongly with temperature and thereby leaving first the recombination as the net reaction, and α decreases. Later, also the recombination rate tends to zero because it is proportional to the square of the density. Hence, $-\frac{d\alpha}{dx}$ approaches rapidly zero in the divergent portion of the nozzle, and α stays constant.

The temperature distribution along the hypersonic nozzle is shown in Figure 4 for both equilibrium and non-equilibrium flow for a supply pressure of 50 atm and for various supply temperatures. The temperature is very much affected by non-equilibrium flow. The ratio between equilibrium to non-equilibrium temperature can reach a factor 4 in certain cases. The reason for it is the fact that the energy of dissociation, which is contained in the gas near the throat, is released step by step in equilibrium flow, while at non-equilibrium flow this energy stays frozen in the gas and does not contribute to the temperature. Because no energy is released in the non-equilibrium flow, this corresponds very close to an adiabatic expansion of a perfect gas, of course with a different γ than for air at standard condition. The temperature distribution for a perfect gas with $\gamma = 1.4$ has been included for comparison.

The Mach number distribution along the hypersonic nozzle is shown in Figure 5 both for equilibrium and non-equilibrium flow for a supply pressure of 10 atm. Because sound velocity is closely related to temperature, the Mach number distributions show similar strong discrepancies between equilibrium and non-equilibrium flow. The ratio of the Mach numbers between the two cases can reach a factor 1.8. It is noted that the Mach number for a perfect gas with $\gamma = 1.4$ is close to the lines of non-equilibrium Mach numbers, which is to be expected in accordance with the discussion of the last figure. It should be observed that the liberation of the dissociated energy by the recombination process in equilibrium flow defeats markedly the purpose of a hypersonic nozzle, namely to produce high Mach numbers by a certain expansion ratio. For non-equilibrium flow fortunately, this undesired effect has been strongly reduced or cancelled.

Pressure and density distributions have also been calculated for the same combinations of supply pressure and temperature. They are not presented here. Pressure is affected similarly, but somewhat less than temperature. The ratio between equilibrium and non-equilibrium flow can reach a factor 3. The density is very little affected, only up to 15%. Investigation of the effect of the length parameter ℓ, which was varied a factor 2.3, onto the flow parameters reveals practically no influence of the nozzle shape or the absolute size of the nozzle, if the flow parameters are compared at a specified area ratio - A/A*. Only a very small decrease in the degree of dissociation (of about 1%) can be observed comparing the shortest and the longest nozzle, that is the longer nozzle assists in the recombination process.

The foregoing results show that there is considerable frozen dissociation in the nozzle flow of most practical hypersonic facilities. This fact is of great importance if a body is placed in to the hypersonic stream, in order to study the simulation of a particular free flight condition. For free flight below 90 km the free stream dissociation in the atmosphere is negligible. Obviously the effect of the frozen dissociation in the stream of the facility on the flow around a body will depend on the fraction of the total enthalpy which is frozen in dissociation, because it might be released behind the shock wave. Hence, the ratio of the frozen enthalpy, h_f to the total enthalpy, h_t, is shown in figure 6 as function of the supply pressure for various temperatures. At supply pressure of 5 or 10 atm about 27% of the total enthalpy is frozen while at 100 atm this fraction drops to 10 or 15%.

4. Non-equilibrium Hypersonic Flow Around Blunt Body

4.1 Inverse and Direct Methods

There are many recent investigations of hypersonic flow with detached shock waves, using both inverse and direct methods. In the inverse method the flow field around the body is determined by specifying a certain shock shape. The associated body shape follows then from the calculation. The problems associated with the specification of boundary conditions along an unknown shock are thus avoided and this method has been successfully applied by Hall, ref. 6, even for real gas flows. The difficulty of the method is that the shock shape must be iterated until a body of the desired shape is produced. Because this goal can be reached only approximately, there is always the open question: how much does the flow around the produced body differ from the flow around the given body.

Recently, Dorodnitsyn, ref. 7, has described an iteration procedure for the solution of two-dimensional boundary value problems. This method is also applicable to problems with free boundaries and has been applied by Belotserkovskii, ref. 8, to the supersonic flow of an ideal gas past a circular cylinder. This basic work has been reviewed by Holt, ref. 9, and expended by various authors, Traugott, ref. 10, for example, but it has not yet been applied to blunt body flows in a real gas.

In this investigation it is attempted to calculate the flow field around blunt bodies in dissociated air by this integral method. The equations are given in the proper form both for the sphere and the circular cylinder. Numerical calculations however are done only for the two-dimensional case of the circular cylinder. They were carried out on the GE-225 computer of the Marshall Space Flight Center at Huntsville, Alabama.

4.2 Basic Assumptions and Equations.

The calculation of the blunt body flow is based on the same assumptions that were given for the nozzle flow (Section 2.1). However, instead of having one independent variable, the flow direction x along the nozzle axis, we have now two independent variables, namely the radial coordinate r and the angular coordinate θ. The polar coordinate system is of course referred to the center of the cylinder. As a consequence, we now have two momentum equations instead of one, namely in the r and θ directions. We have now five equations, namely for continuity, radial and angular momentum, energy, and rate of dissociation. They all can be written as partial

differential equations in r and θ in the following form:

$$\frac{\partial F}{\partial r} + \frac{\partial G}{\partial \theta} + H = 0 \qquad (27)$$

where F, G, and H are functions of all the flow variables.

Before equation (27) can be integrated between the shock and the body surface, the conditions for the flow variables across the shock have to be determined. Afterwards we have to find expressions for the derivatives of all flow variables immediately behind the shock with respect to θ. These derivatives are calculated under the following assumptions:

a) the shock is assumed to be locally an oblique shock.

b) the chemical composition of the gas does not change across the shock, that is we assume frozen dissociation

c) for hypersonic flow there is $P_\infty \ll \rho_\infty U_{n\infty}^2$,

d) the contribution of the free stream temperature to the enthalpy can be neglected, not, however, the energy bound in the free stream dissociation.

4.3 Application of Belotserkovskii's Method for the Flow Past a Circular Cylinder.

Having reduced the equations of motion to the form of eq. 27, Belotserkovskii's method consists essentially of transforming the partial differential equations with two independent variables into ordinary differential equations with one variable. Integrating equation 27 with respect to r between the body surface (r_b) and the shock surface (r_s) we get

$$(F)_s - (F)_b + \int_{r_b}^{r_s} \frac{\partial G}{\partial \theta}\, dr + \int_{r_b}^{r_s} H\, dr = 0 \qquad (28)$$

Using Leibniz's formula for differentiating integrals, the second term on the left hand side can be rewritten and this equation becomes

$$(F)_s - (F)_b + \frac{d}{d\theta} \int_{r_b}^{r_s} G\, dr - (G)_s \frac{dr_s}{d\theta} + \int_{r_b}^{r_s} H\, dr = 0 \qquad (29)$$

In order to integrate the equations of this form all integrands are now approximated by means of an interpolation polynomial in r. In our case, only a first order polynomial is used and therefore the procedure is called the first approximation. Substituting the polynomial, introducing a dimensionless shock detachment distances ϵ and performing the integration, all equations assume the form of

$$(F)_s - (F)_b + \frac{r_b}{2}\frac{d\epsilon}{d\theta}\left[(G)_b + (G)_s\right] + \frac{\epsilon r_b}{2}\frac{d}{d\theta}\left[(G)_s - (G)_b\right]$$

$$+ \frac{\epsilon r_b}{2}\left[(H)_s - (H)_b\right] = 0 \qquad (30)$$

We are using now the previously established shock transition conditions and their derivatives behind the shock with respect to θ. We apply these relations to the previously mentioned five equations of motion, in addition to the equation of state and add a simple geometric relation between the shock detachment distance ϵ and the shock angle σ . Those seven equations are now brought into the final form of the following equation which is given as a sample.

$$\phi_1 \frac{du_{\theta b}}{d\theta} + \phi_2 \frac{d\rho_b}{d\theta} + \phi_3 \frac{dp_b}{d\theta} + \phi_4 \frac{dT_b}{d\theta} + \phi_5 \frac{d\sigma}{d\theta} + \phi_6 \frac{d\alpha_b}{d\theta} + \phi_7 = 0 \qquad (31)$$

The ϕ's are functions of all the thermodynamic and gas dynamic variables. In total, we have seven ordinary differential equations for the seven unknowns $u_{\theta b}$, ρ_b, p_b, T_b, σ, α_b, and ϵ which are simultaneously solved by the computer.

4.4 Numerical Calculation Procedure

For the actual calculation procedure all our differential equations are made dimensionless by relating the variables to their corresponding free stream values. The conditions behind the shock at each value of θ are calculated from the oblique shock relations. It is also assumed that the flow is in equilibrium at the stagnation point. This assumption seems to be justified due to the fact that the particles which are flowing exactly on the stagnation stream line, move very slowly when approaching the stagnation point. Hence, there should be sufficient time to reach equilibrium. However, after obtaining the numerical results of the calculation, it seems that this assumption is somewhat artificial, and it would be better to use the frozen flow as initial condition.

The numerical procedure consists of two parts. First, for every value of θ, the derivatives of all the variables are calculated from the set of simultaneous differential equations by using determinants. Then the derivatives are integrated simultaneously by the Runge-Kutta integration method. It should be noted that the equations do not readily yield the shock detachment distance on the stagnation

stream line. In order to find ϵ_o, a very tedious iteration procedure has to be used. A tentative value for ϵ_o is selected, then the integration must be carried out over the whole range of θ towards the sonic point. If the selected ϵ_o is either too large or too small compared to the "correct" value, the velocity, when plotted versus θ will have either a horizontal or a vertical tangent. Theoretically, this iteration has to be continued until an ϵ_o is found such that the velocity reached local Mach number one, and that the derivatives of all the variables are continuous across the sonic line. In practice one finds that, approaching the sonic point, the equations become so sensitive that the velocity as well as the other flow parameters (p, ρ, T, α) may start to oscillate. The ϵ_o must be varied to the third or fourth significant figure (better than 0.1%), to come close to the sonic point. In order to keep the computation time to a reasonable value, we had to stop the calculation when reaching about 0.98 of the sonic velocity. The variables then were extrapolated to the sonic point with their respective tangents.

The difficulties encountered are typical for trying to apply a numerical solution near a saddle point. Authors who have applied the Belotserkovskii method even to the flow of a perfect gas with much simplified conditions with respect to enthalpy and rate equation have found the same difficulties.

4.5 Discussion of the Numerical Results of the Non-equilibrium Flow Past a Circular Cylinder.

Numerical results have been obtained so far only for one set of free stream conditions because of the limited time during which the computer is available and the length of time needed to produce the solution. The wind tunnel reservoir conditions are p_t = 10 atm, T_t = 5000°K, at a nozzle cross section, where the frozen Mach number is M_f = 14.91. This corresponds to a free stream velocity U_∞ = 3,665 m/sec and a frozen free stream degree of oxygen dissociation α_∞ = 0.70. These conditions were chosen in order to show a distinct effect on non-equilibrium flow in a wind tunnel nozzle compared to the flow field around a blunt body.

The calculated shock pattern around the cylinder is shown in Figure 7. The dimensionless shock detachment distance is ϵ_o = 0.655, which is considerably larger than that of perfect gas flow. The shock is much blunter than the concentric circle through the shock detachment point. The sonic point has been determined to be at about 30°. The last reliable point in the velocity calculation was at θ = 28.6°. From here, all the curves were extropolated to the sonic velocity.

The oxygen dissociation on the non-reacting surface of the cylinder is shown in Figure 8. The equilibrium dissociation at the stagnation point is practically 1.00. Calculations show that the dissociation drops immediately, i.e. within about one degree, to a value which is very close to the free stream frozen value. Then the dissociation stays nearly constant. The sharp drop from the assumed equilibrium value to the free stream frozen value indicates that the assumption of equilibrium condition at the stagnation point is artificial and that the dissociation occuring at the body, only slightly away from the stagnation point, is determined by the frozen dissociation behind the shock. The frozen dissociation is carried through the thin shock layer to the body. A recombination of oxygen along the body does not occur. Equilibrium flow calculations, by the same method as used by us in ref. 11, show the same behavior, that is, nearly no change in dissociation. Pressure, temperature, and density distribution have been calculated but are not shown here. The pressure distribution lies somewhat below the modified Newtonian theory as previously shown by other authors using the inverse method, for instance Hall (ref. 3, 6). The velocity distribution along the cylinder surface, as evident in Figure 9, shows first an approximately linear behavior and then an increasing slope. The velocity distribution calculated for equilibrium condition and potential flow, ref. 1, is rather close.

5. Conclusions

We have investigated high enthalpy, non-equilibrium nozzle flow of air. Results are given for supply temperatures of 4000 to 6000^{o}K and for supply pressures of 10 to 100 atmospheres. It is concluded that high temperature air flow in hypersonic wind tunnels is frozen beyond a cross section where Mach number 2 or 3 is reached, because of the rapid expansion of the gas downstream of the nozzle throat. This means that the chemical composition of the gas remains constant in the hypersonic portion of the nozzle. This freezing has a strong effect on the temperature, the Mach number, and on the pressure, but vanishing effect on the density distribution along the nozzle.

The flow field around a circular cylinder up to the sonic point, the shock shape and the shock detachment distance have been determined by the direct method. Shock shape and detachment distance are very much affected by the frozen free stream dissociation, i. e., the shock moves further upstream and the shape deviates considerably from a concentric circle. The degree of dissociation is

markedly different from that for equilibrium flow.

The flow in the hypersonic nozzle and around the cylinder have been treated considering only the oxygen dissociation of the air. The equations, however, can easily be modified to calculate non-equilibrium flow at such elevated temperatures where nitrogen dissociation is encountered. Because the oxygen is completely dissociated before the nitrogen dissociation starts, we have a similar separation of the dissociation of the two species as treated in this paper. Some complexity will be added due to the fact that both types of dissociation may occur at the same time in one flow field, but of course in two different areas.

The results of this investigation shed light on the problems that are connected with the simulation of free flight conditions in a hypersonic wind tunnel. Below a certain altitude (about 90 km) a re-entering body does not encounter appreciable free stream dissociation in the Earth's atmosphere. Hence, if such altitudes shall be simulated in the wind tunnel under supply conditions that very probably will cause dissociation, extreme care has to be used in interpreting the observed flow parameters. We are aware that this investigation is only a first step and many similar investigations have to follow. In particular this method should also be applied to flow fields around blunt bodies of various shapes, in particular to axi-symmetric bodies such as spheres, ellipsoids, or nose cones.

REFERENCES

1. Hermann, R. -- Hypersonic Flow Problems During Re-Entry into the Atmosphere. Proceedings of the Annual Meeting at Freiburg, Germany, October, 1961. Jahrbuch 1961 der Wissenschaftlichen Gesellschaft fuer Luftfahrt, pp. 131-144. F. Vieweg & Sohn, Braunschweig, 1962.

2. Emanuel, G. and Vincenti, W. G. -- Method for Calculation of the One-Dimensional Non-Equilibrium Flow of a General Gas Mixture through a Hypersonic Nozzle. AEDC Tech. Doc. Report AEDC-TDR-62-131, June, 1962.

3. Hall, J. G., Eschenroeder, A. Q. and Boyer, D. W. -- Exact Solutions for Non-Equilibrium Expansions of Air with Coupled Reactions. AFOSR-622, May, 1961

4. Hansen, C. F. -- Approximations for the Thermodynamic and Transport Properties of High Temperature Air. NASA-TR-R-50, 1959.

5. Glowacki, W. J. -- Effect of Finite Oxygen Recombination Rate on the Flow Conditions in Hypersonic Nozzles. NOLTR-61-23, September, 1961.

6. Hall, J. G. -- Inviscid Hypersonic Air Flows with Coupled Non-Equilibrium Processes. Cornell Aero. Lab Report No. AF-1413-A-2; also, AFOSR-2072, May, 1962.

7. Dorodnitsyn, A. A. -- A Contribution of the Solution of Mixed Problems of Transonic Aerodynamics. "Advances in Political Sciences"; Vol. 2, New York Pergamon Press, 1959.

8. Belotserkovskii, O. M. -- Flow Past a Circular Cylinder with a Detached Shock Wave. Doklady AN USSR, Vol. 113, No. 3, 1957 (Translation available from Morris D. Friedman, Inc., Needam Heights, Mass.). AVCO, Tech. Memo. RAD- 9-TM-59-66, September, 1959.

9. Holt, M. -- Calculation of Pressure Distribution on Hypersonic Bodies of Revolution by Belotserkovskii's Method. AVCO Technical Memorandum RAD-2-TM-58-45, September, 1958.

10. Traugott, S. C. -- An Approximate Solution of the Supersonic Blunt Body Problem for Prescribed Arbitary Axi-Symetric Shapes. Martin Company Research Report No. 13, August, 1958.

11. Hermann, R., Thompson, K. and J. Yalamanchili -- An Analytical Study of the Effects of Dissociation of High Temperature Air at Hypersonic Velocities around Blunt Bodies and Study of Design Requirements of Arc Heated Hypersonic Wind Tunnels. Rosemount Aeronautical Laboratories Research Report No. 185, August, 1962.

12. J. Yalamanchili, Hermann, R. -- Non-Equilibrium Hypersonic Flow of Air in Hypersonic Nozzles and Around Blunt Bodies. University of Alabama Research Institute Research Report No. 3, May, 1963.

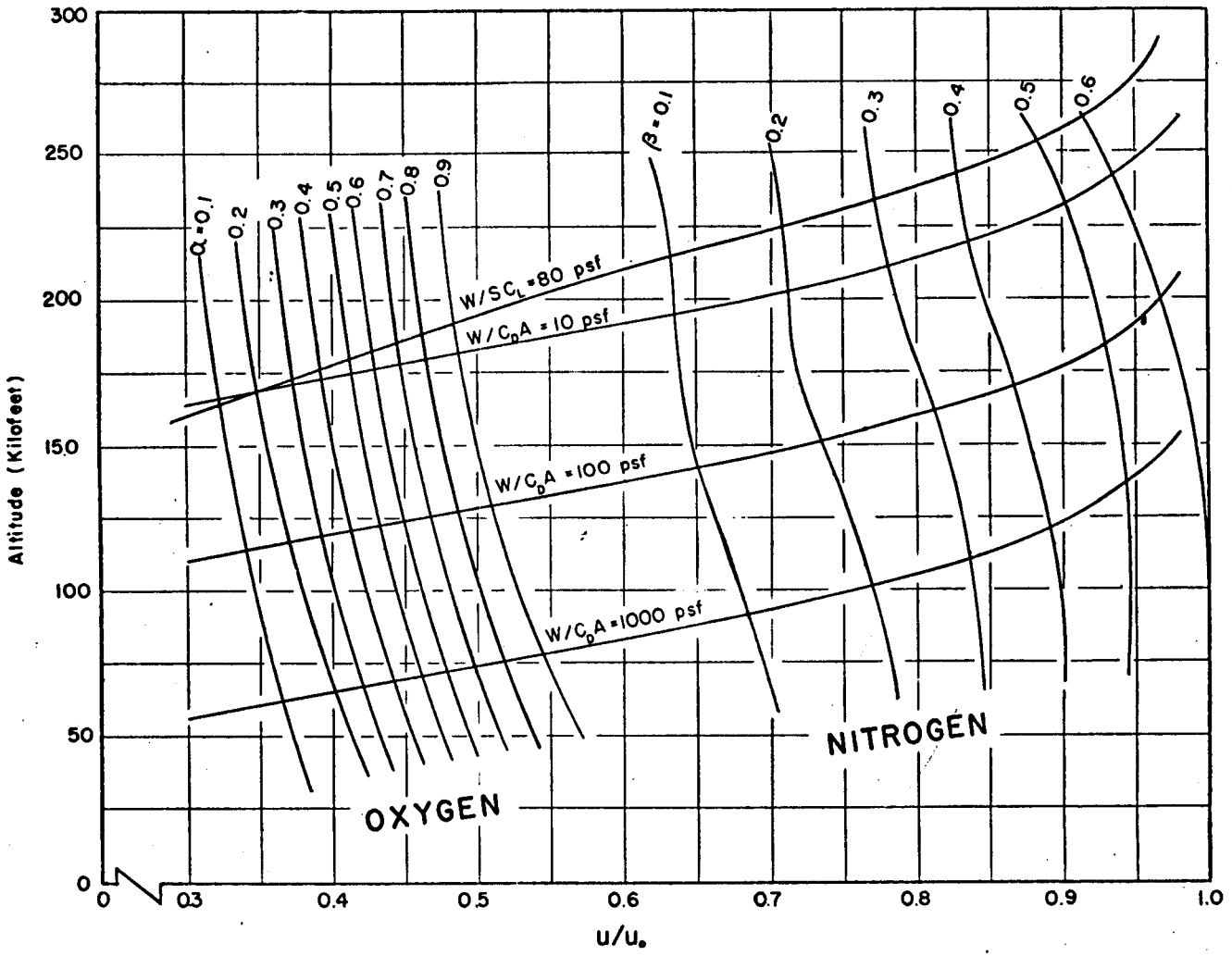

FIGURE 1. DEGREE OF OXYGEN AND NITROGEN DISSOCIATION FOR SIMPLIFIED AIR-MODEL AT STAGNATION POINT IN ALTITUDE VS VELOCITY DIAGRAM; ALSO RE-ENTRY TRAJECTORIES FOR VARIOUS BALLISTIC AND GLIDE VEHICLES. (W/C_DA = 10, 100, 1000 lb/ft^2 AND W/SC_L = 80 lb/ft^2)

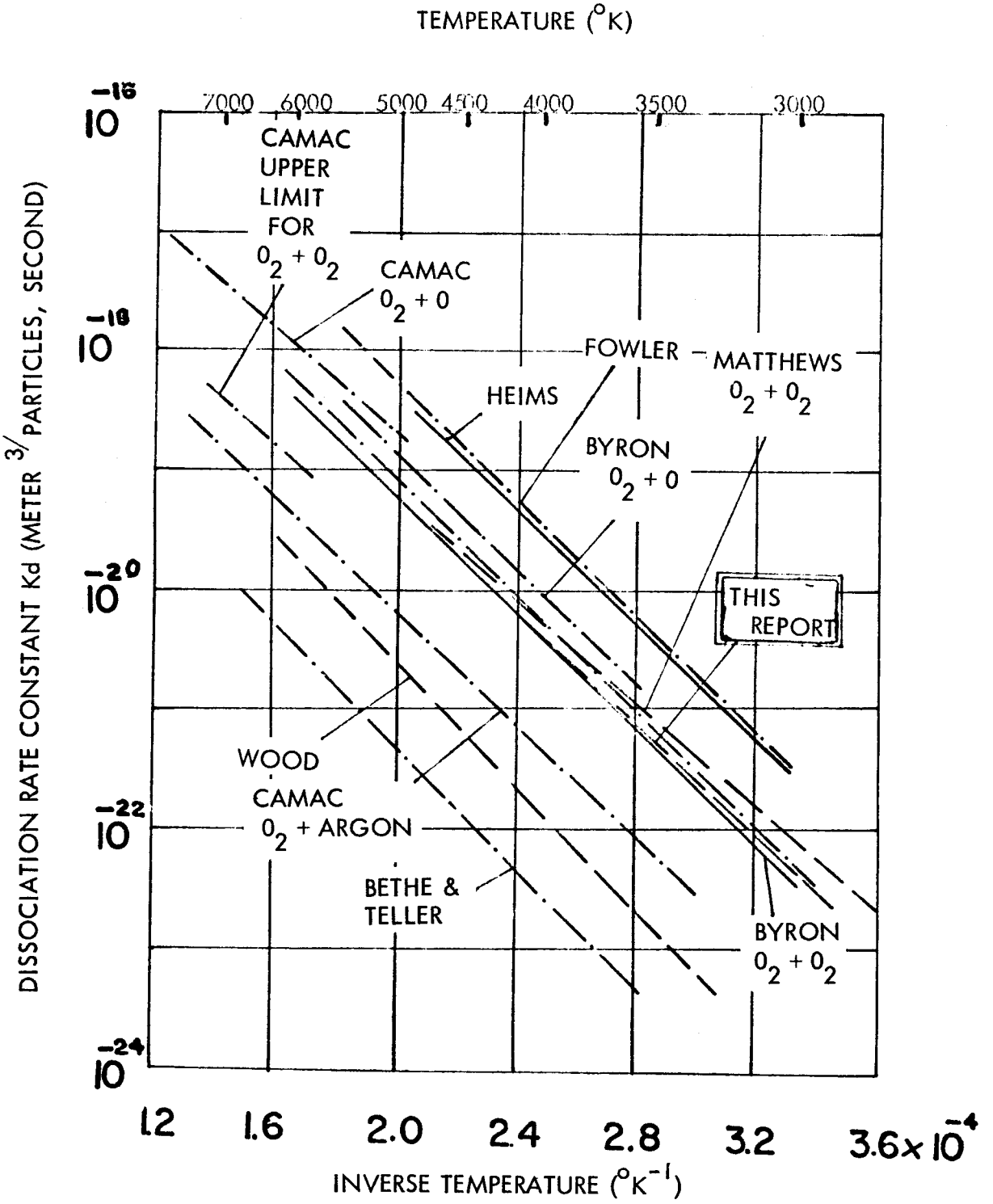

FIG. 2 OXYGEN DISSOCIATION RATE CONSTANT FOR VARIOUS COLLIDING BODIES, OTHER AUTHORS AND THIS REPORT

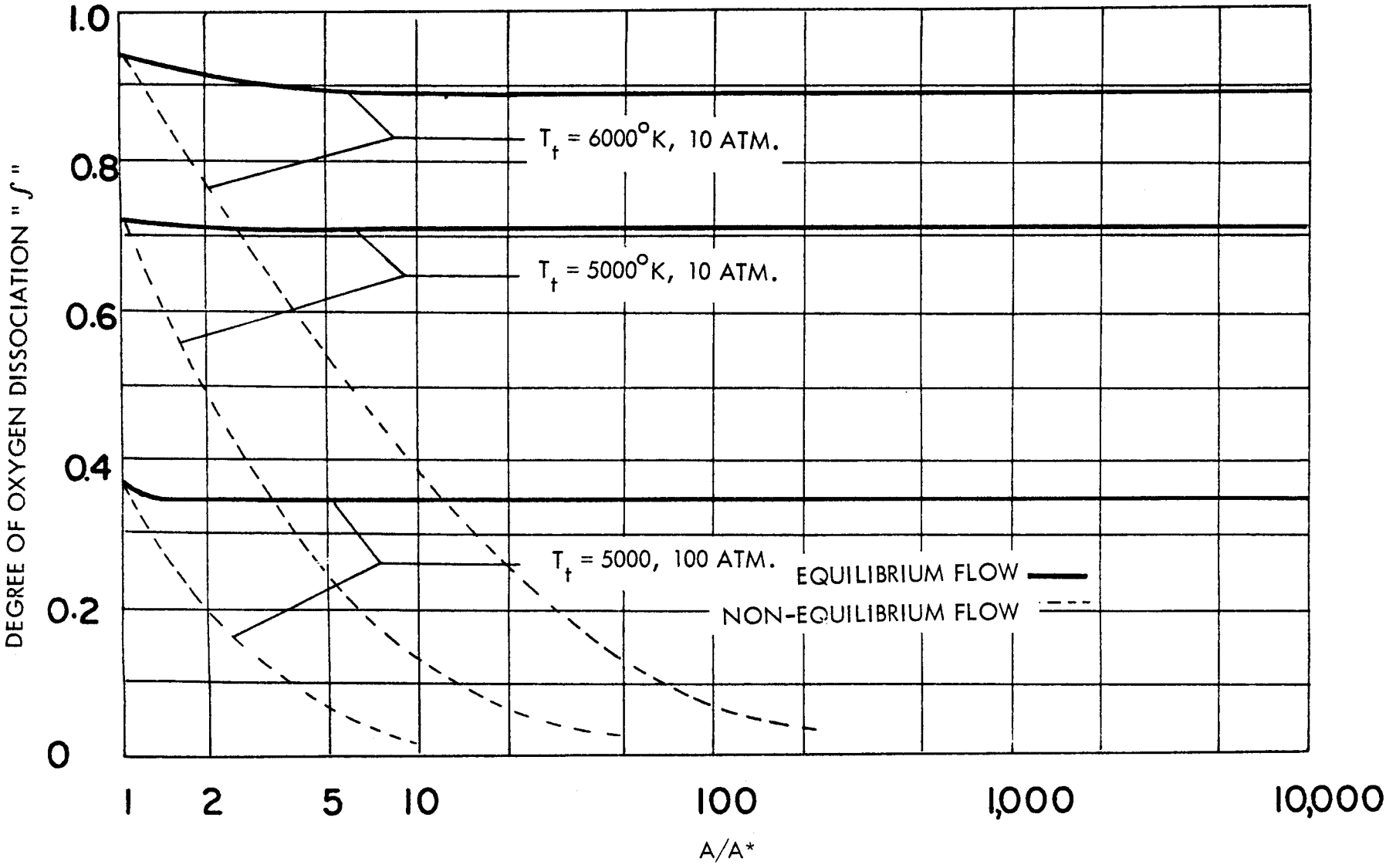

FIG. 3 DEGREE OF OXYGEN DISSOCIATION ALONG HYPERSONIC NOZZLE IN EQUILIBRIUM FLOW AND NON-EQUILIBRIUM FLOW

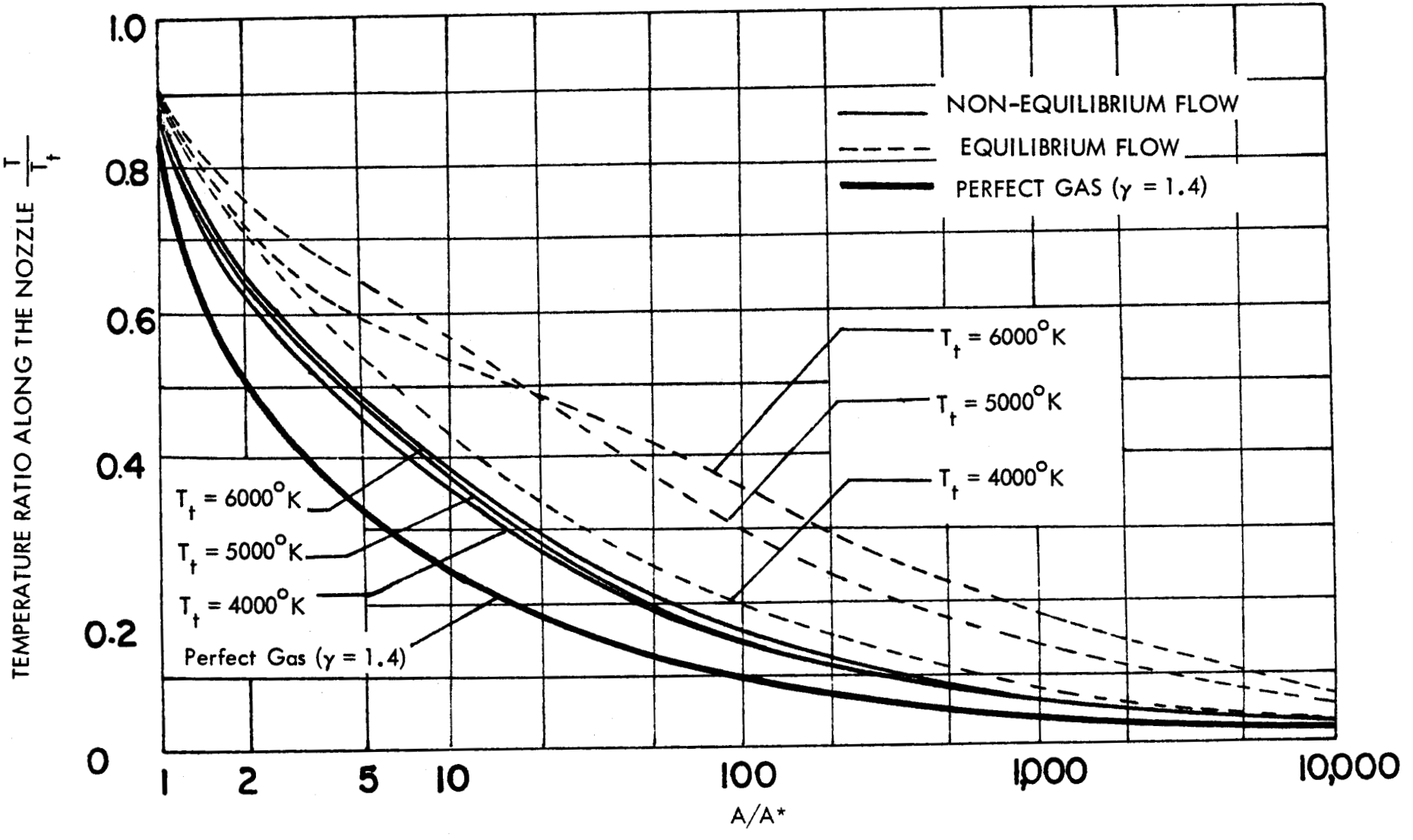

FIG. 4 TEMPERATURE DISTRIBUTION ALONG THE HYPERSONIC NOZZLE IN EQUILIBRIUM AND NON-EQUILIBRIUM FLOW FOR P_t = 50 atm.

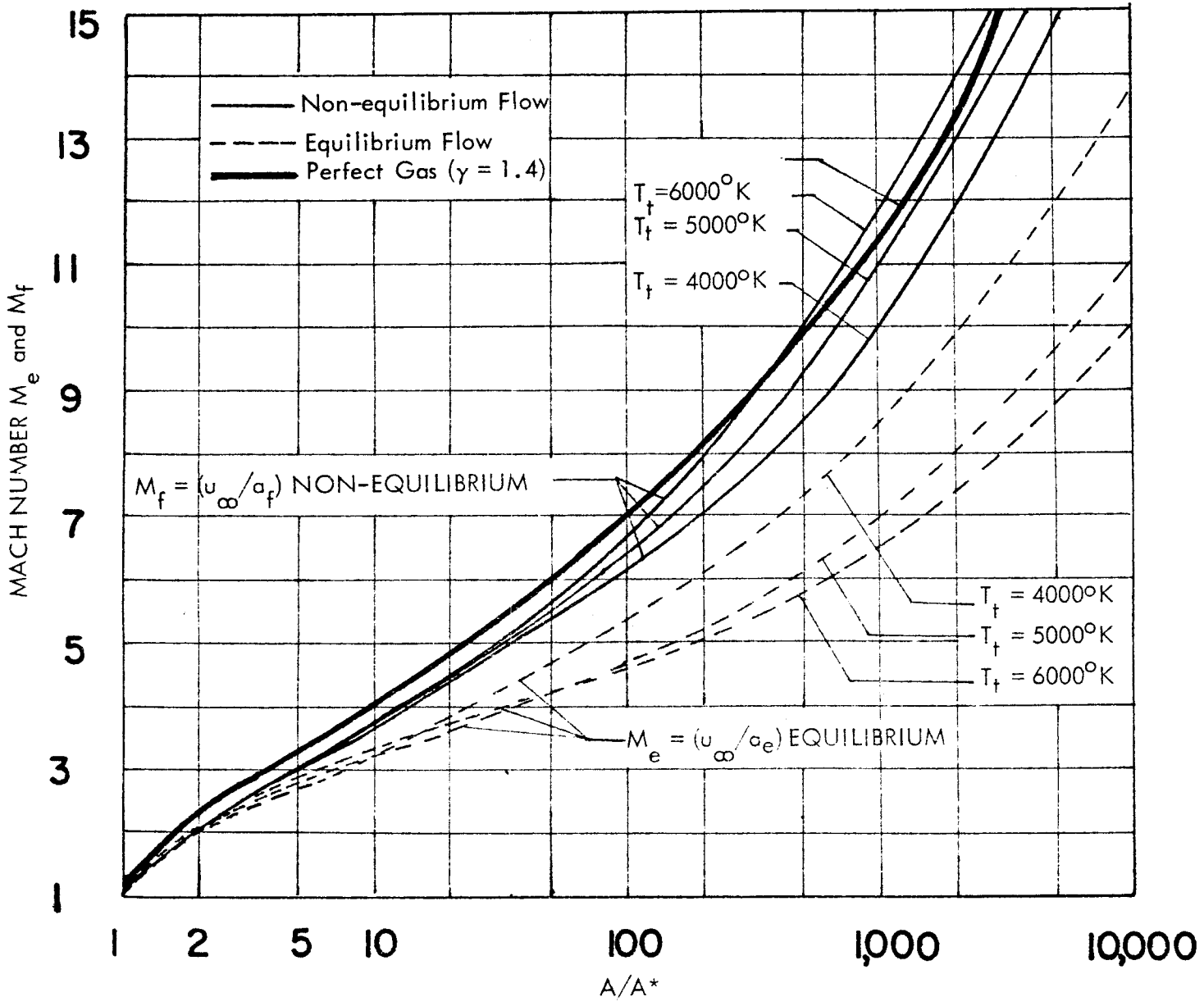

FIG. 5 DEGREE OF OXYGEN DISSOCIATION ALONG HYPERSONIC NOZZLE IN EQUILIBRIUM AND NON-EQUILIBRIUM FLOW

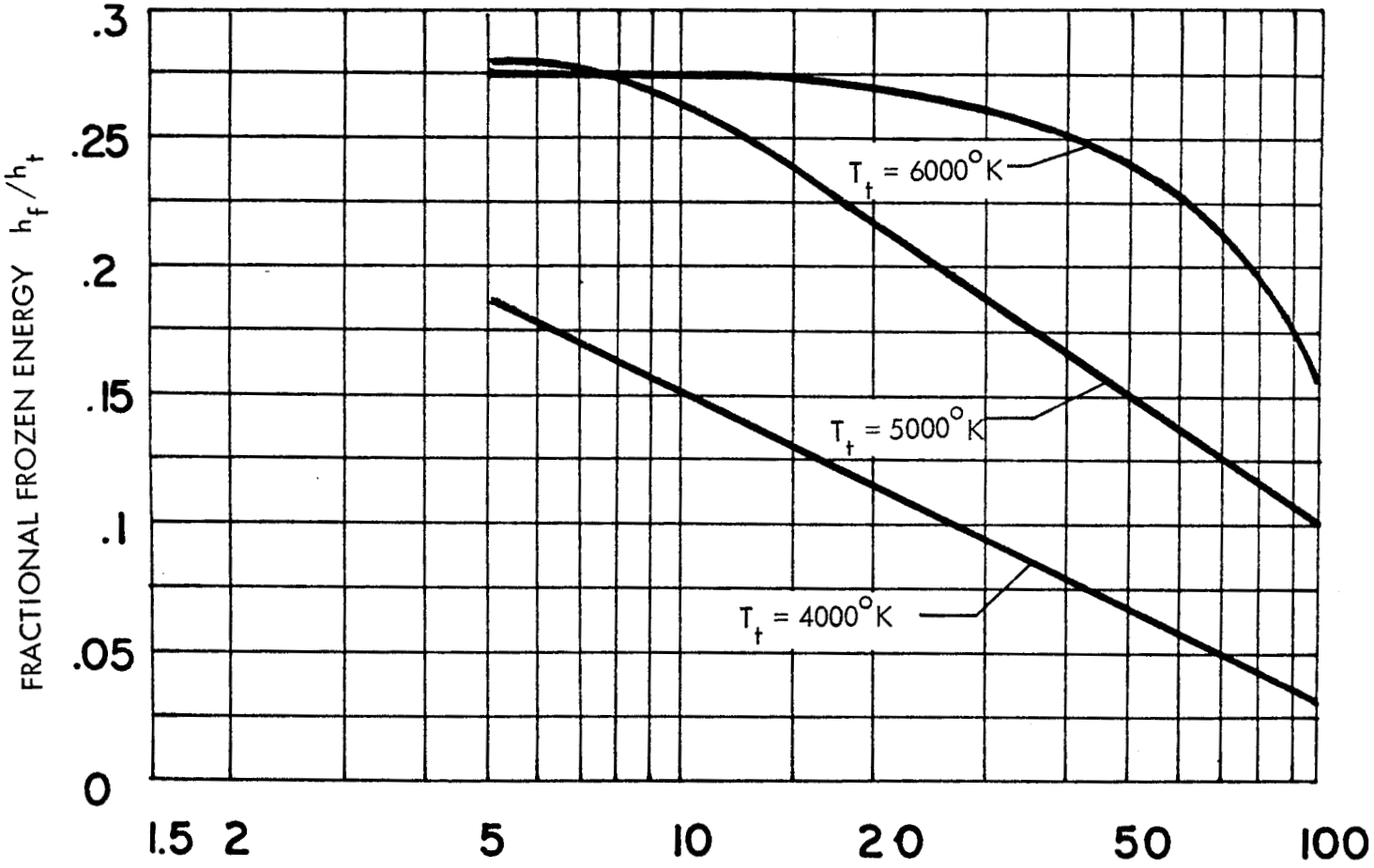

FIG. 6 FROZEN ENERGY FRACTION IN HYPERSONIC NOZZLE AS A FUNCTION OF STAGNATION PRESSURE

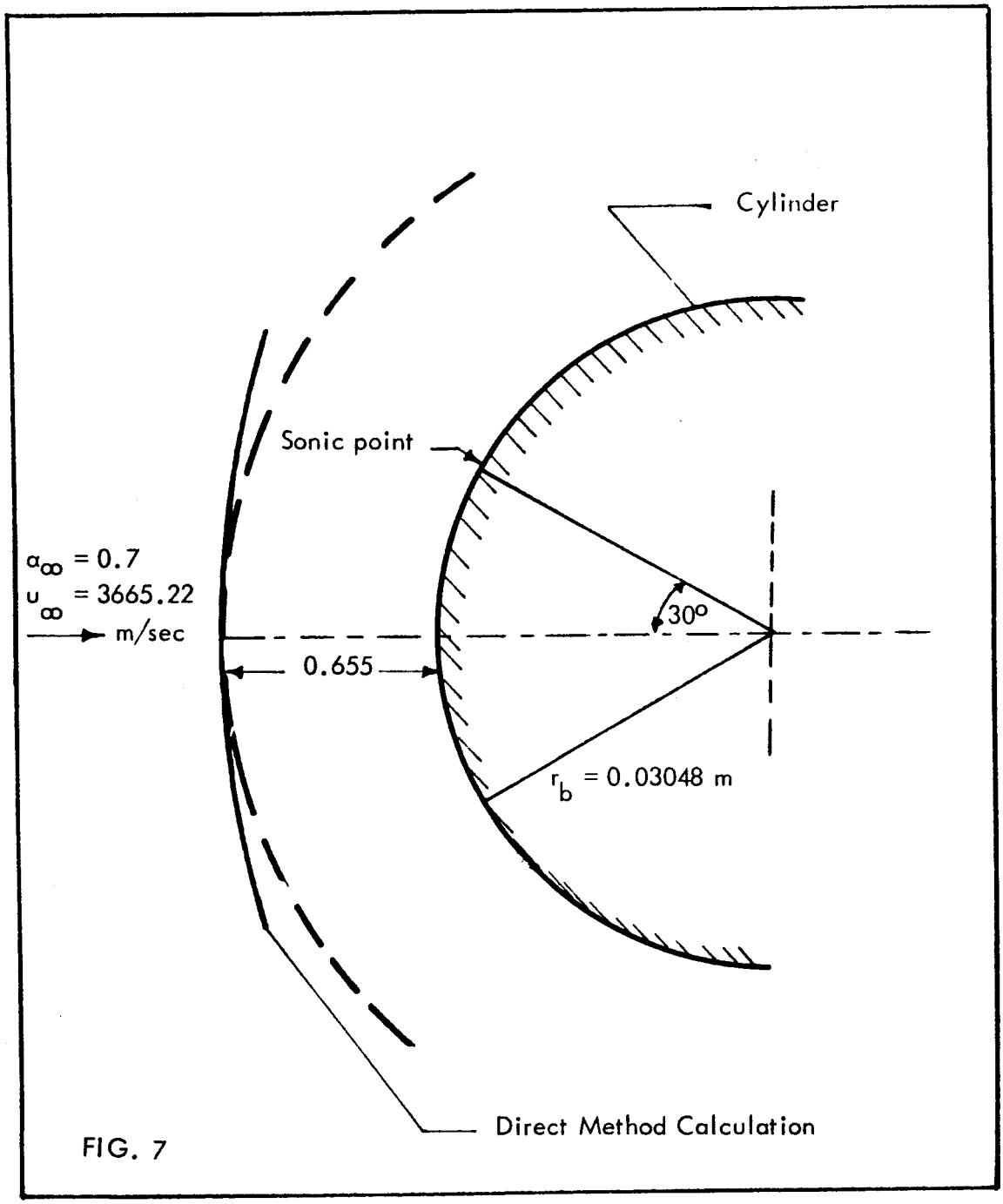

FIG. 7

CALCULATED SHOCK SHAPE BY DIRECT METHOD FOR NON-EQUILIBRIUM AIR FLOW AROUND A CYLINDER IN HYPERSONIC WIND TUNNEL. ($M_f = 14.91$, $P_t = 10.1325$ bar, $T_t = 5000^\circ K$)

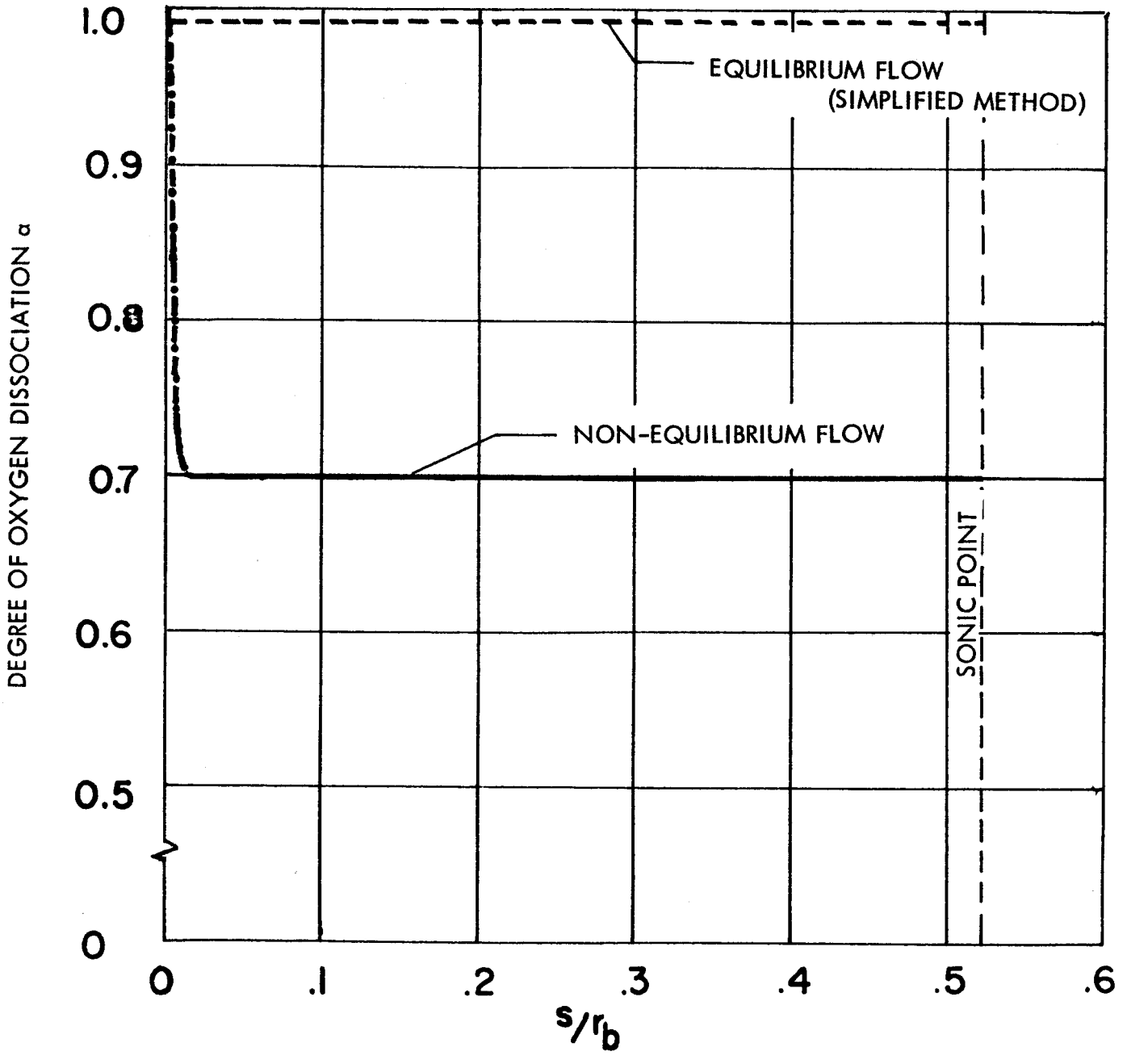

FIG. 8 OXYGEN DISSOCIATION IN HYPERSONIC FLOW ON THE NON-REACTING SURFACE OF A CYLINDER IN A HYPERSONIC WIND TUNNEL ($M_f = 14.91$, $P_t = 10$ atm., $T_t = 5000^{\circ}K$)

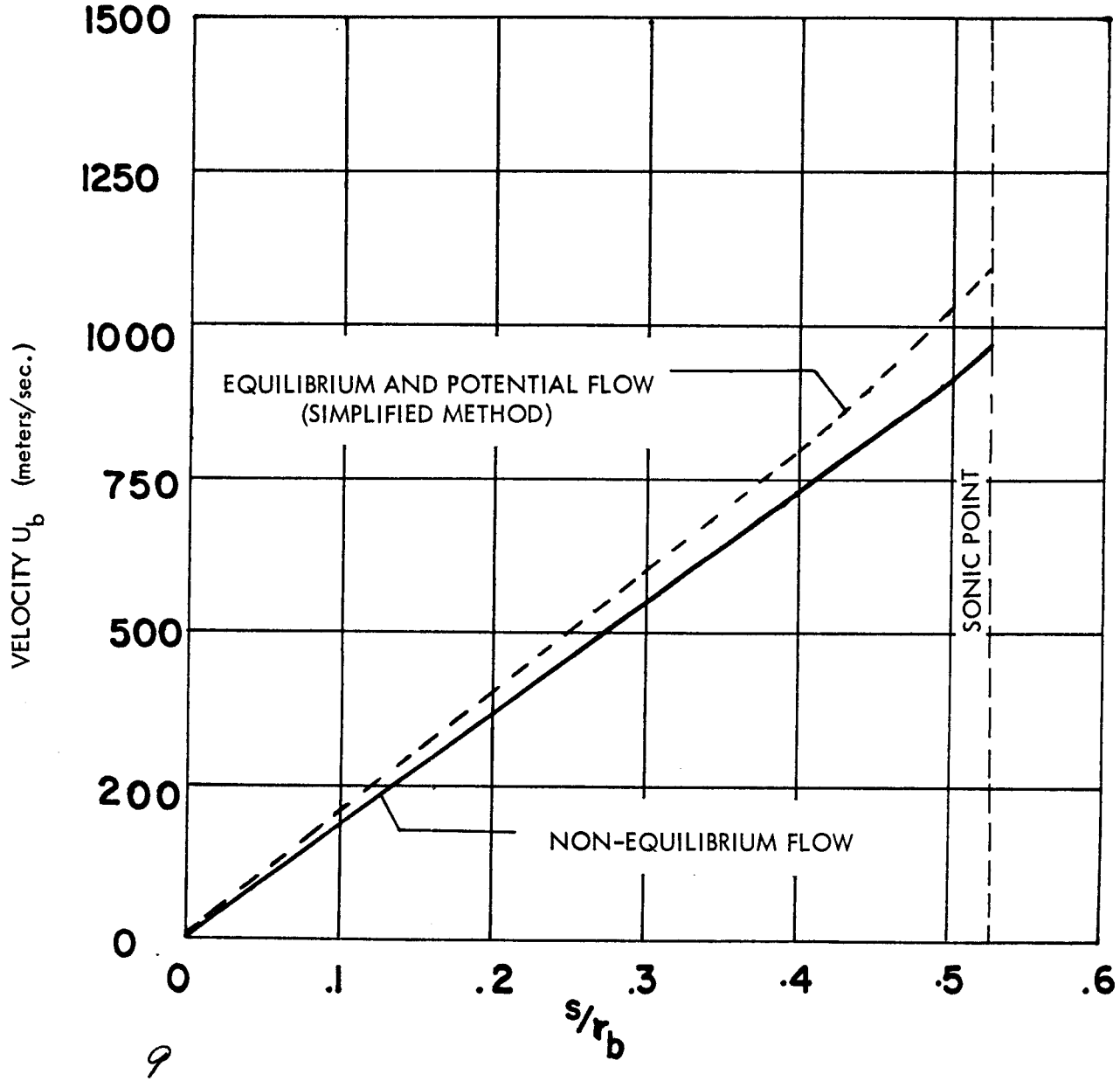

FIG. 9

VELOCITY DISTRIBUTION IN HYPERSONIC FLOW ON THE NON-REACTING SURFACE OF A CYLINDER IN A HYPERSONIC WIND TUNNEL
(M_f = 14.91, P_t = 10 ATM, T_t = 5000°K, U_{oo} = 3665 meters/sec)